



Selection of Multi-layer Remote Phosphor Structure for Heightened Chromaticity as well as Lumen Performance within WLED Devices

Phuc Dang Huu^{1*}, Dieu An Nguyen Thi²

¹*Institute of Applied Technology, Thu Dau Mot University, Binh Duong Province, Vietnam*

²*Faculty of Electrical Engineering Technology, Industrial University of Ho Chi Minh City, Ho Chi Minh City, Vietnam*

Abstract. The hue output for remote phosphor layout is still a concern for researchers and producers working on developing WLED devices since said layout proves inferior to the conformal or in-cup phosphor package. However, the luminous efficiency in the layout showed significant improvements. Thus, this study aims to achieve higher color quality accompanied by high lumen output for remote phosphor structures by using additional phosphor layers. Specifically, the study introduces the double-film and triple-film configurations in which the red and green phosphors were added. The best structure for WLED applications is determined by comparing these structures. The influences of each phosphor structure are investigated and examined on optical parameters of WLEDs, which have different correlated hue temperatures between 5600 K and 8500 K. The optical features are CRI, CQS, color deviation (CD), and photoluminescence (PL). The results demonstrate that the triple-layer structure improved the color quality more effectively than the dual-layer structure due to higher attained CRI and CQS and smaller DC figures. The hypothesis of Mie-scattering indicates that the enhancement of scattering in the triple-layer is responsible for these achievements. Thus, the findings of this study are reliable and valuable for manufacturers.

Keywords: Color quality; Color quality scale; Color rendering index; Luminous efficiency; Remote phosphor structure; Triple-layer phosphor structure; WLEDs

1. Introduction

Light-emitting diodes (LEDs) have laid the concrete foundation for their widespread usage in the solid-state lighting (SSL) industry (Sulistiyanto et al., 2014; Widiyati et al., 2018). They can especially be served as an alternative solution to halogen, incandescent, and fluorescent illuminating systems since they are safer and sturdier. Researchers also pointed out that LEDs potentially have better energy conversion efficiency leading to less heat release, longer lifetime, and more stable brightness performance (Nguyen et al., 2021a; Luo et al., 2020). A LED package was conventionally fabricated utilizing the synthetic of a blue chip and a yellow phosphor material. Thus, the generated light of LED was comprised of blue and yellow lights from these two elements (Anh et al., 2017b). The freely dispersed phosphor coating is one of the most simple and massively applied techniques for manufacturing WLEDs. The mixture of phosphor particles and silicone was spread freely above the bare blue chip.

*Corresponding author's email: danghuuphuc@tdmu.edu.vn; Tel.: +84-09-09041387, Fax. +84-09-09041387
doi: [10.14716/ijtech.v13i4.5051](https://doi.org/10.14716/ijtech.v13i4.5051)

The advantages of using said method were adjustable phosphor layer thickness and low cost, yet the disadvantage is the poor optical performance of the LED package. Therefore, it is inappropriate to produce high-power WLEDs (Jiang et al., 2017; Yang et al., 2019b; Yuce et al., 2019). The conformal phosphor coating was then introduced to improve the quality of LEDs. Even though this method effectively enhanced the color uniformity due to its ability to provide uniform color distribution, the backscattering in the package caused degradation in light extraction efficiency (Yang et al., 2019a; Ding et al., 2018; Gao et al., 2018). Additionally, these methods directly placed the phosphor layer onto the LED chip surface, stimulating caustic at the joint and reducing the phosphor's efficiency and the lifetime of the LED device. Hence, researchers devised the idea of creating a gap or adding another film between the main phosphor-silicone encapsulation and the LED chip to improve light extraction and minimize heat generation (Anh et al., 2020; Zhang et al., 2016). This structure was called the remote phosphor structure, and it fastly became a popular topic in various studies of enhancements for WLEDs' optical properties. A thermal-isolated encapsulation was designed to increase the light output power by controlling heat generation during the high operation time of a WLED (Li et al., 2016). The light extraction efficiency of the remote phosphor package was improved using various approaches, including internal reflection enhancement by employing the innerphosphor-coated polymer hemispherical shell lens, downward-light reflection by the airgap embedded structure, and backscattered-light reduction by the ring remote phosphor structure (Ge et al., 2015). To create a high-grade WLED, aside from the essential light extraction efficiency, another decisive factor is color quality, including CRI and CQS. The study introduced the layout with two sheets to improve chromatic adequacy and luminous efficiency. It was shown that by using the remote phosphor structure with two phosphor layers, the WLED package could improve its lumen output by 5% and color uniformity by offering a significant reduction in the angular color deviation (Thon et al., 2021). However, the performance of a dual-layer phosphor package is usually determined by the phosphor layer that has been added. Notably, with a red phosphor layer, CRI figures can be improved, but the luminous flux is degraded, and vice versa in the case of using green phosphor. Besides, according to previous studies, the growth in phosphor concentration led to a higher reabsorption loss in the package, which decreased the luminous flux (Cheng et al., 2019; Anh et al., 2017a). Then, the concept of using one more phosphor layer can be potential consideration. The triple-film distant phosphor configuration was proposed with the participation of the yellow, green, and red phosphor films. The first film is the yellow phosphor, which is closest to the LED chip, the second film is the green phosphor, and the third film is the red phosphor. In this study, the authors concentrate on the performance of triple-layer remote phosphor film on the illumination effectiveness of the WLED. Phosphor concentrations are also adjusted to observe and analyze changes in the packages of light extraction, emission spectra, color deviation, CRI, and CQS (Davis & Ohno, 2010). Furthermore, the comparison among the single-layer, two-sheet, and three-sheet remote layouts is presented to prove that using the three-film remote design is more beneficial to the quality of LED. The phosphors used to fabricate the phosphor packages in the article are yellow phosphor YAG: Ce³⁺, red phosphor CaO: Eu³⁺, and green phosphor Zn₂SiO₄:Mn²⁺. In addition, the authors apply the hypothesis of Mie scattering and the law of Lambert-Beer to the measurements. Thus, the outcomes in this study are more reliable and can assist manufacturers in determining the most suitable remote phosphor package to accomplish their goals in high-power WLED production.

2. Research Method

2.1. WLED Modeling

By applying the commercial software of LightTools 9.0, researchers can successfully carry out the simulation modeling of four remote-phosphor-layer structures: a single film

remote phosphor, two dual-film distant phosphor packages with red and green phosphors, and a triple-film one, respectively, as shown in Figure 1 (c) – (f). The enhancement of the chromaticity can be accomplished with the increase of the red spectra by using red phosphor CaO:Eu^{3+} . Meanwhile, green elements in the white-light spectral power band can be boosted with $\text{Zn}_2\text{SiO}_4\text{:Mn}^{2+}$ green phosphors to acquire higher and more stable luminous efficacy for the WLED.

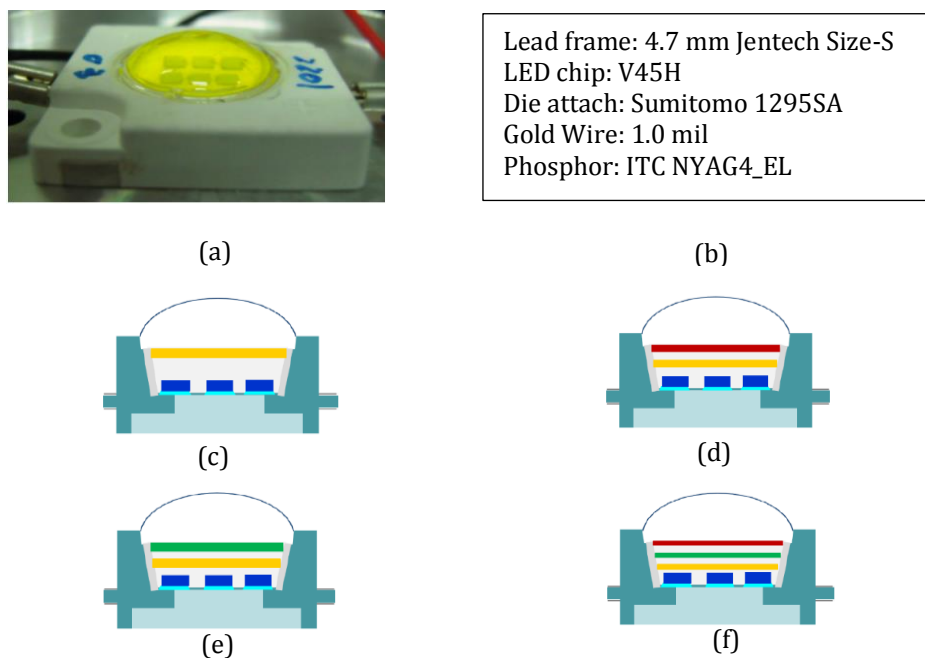


Figure 1 The schematic illustrations of (a) The real WLED, (b) the devices' information, (c) Single-film remote configuration (Y), (d) Dual-film remote configuration with red phosphor CaO:Eu^{3+} (YR), (e) Dual-film remote configuration with green phosphor $\text{Zn}_2\text{SiO}_4\text{:Mn}^{2+}$ (YG), (f) Triple-layer remote configuration (YGR)

Figure 1 (a) demonstrates that the WLED sample used in this modeling process is the multi-chip WLED in which nine blue chips are attached to the lead frame. The chip properties, in this case, are 1.16W radiant power and 453 nm peak wavelength. Figure 1 (b) shows detailed information about the WLED sample. Figure 1 (c) illustrates that the yellow phosphor YAG:Ce^{3+} layer (Y) was used in the single-film distant phosphor configuration. Figure 1 (d) shows dual-film using yellow phosphor and additional red phosphor $\text{CaCO}_3\text{:Eu}^{3+}$ (YR), while Figure 1 (e) displays yellow and green $\text{Zn}_2\text{SiO}_4\text{:Mn}^{2+}$ phosphor layers (YG). Figure 1 (f) depicts a diagram of the triple-layer structure simulation using green and red phosphor layers (YGR). The green phosphor is the intermediate layer, and the red phosphor is the top sheet.

The optical analysis was carried out on these four structures at five different correlated color temperatures (CCTs) of 5600 K, 6600 K, 7000 K, 7700 K, and 8500 K, with different concentrations of red and green phosphors. As the concentrations change, the YAG:Ce^{3+} concentration needs adjustment to ensure the stability of the CCTs, leading to variations in phosphor concentration and scattering ability of each package.

2.2. Preparing Red and Green Phosphor Materials

Phosphor preparation is extremely important to a successful WLED simulation. Tables 1 and 2 show the compositions of the red $\text{CaO}_3\text{:Eu}^{3+}$ and green $\text{Zn}_2\text{SiO}_4\text{:Mn}^{2+}$ (Agarwal et al., 2017). The process of preparing these phosphors can be carried out as follows.

Table 1 Constituents for red phosphor $\text{CaO}_3:\text{Eu}^{3+}$

Ingredient	Mole (%)	By weight (g)
CaCO_3	100	100
CaF_2	1.5	1.2
Eu_2O_3	1.2 (of Eu)	2.1

Table 2 Constituents for red phosphor $\text{Zn}_2\text{SiO}_4:\text{Mn}^{2+}$

Ingredient	Mole (%)	By weight (g)
ZnO	194	158
SiO_2	110	66
MnCO_3	6	6.9

The red phosphor $\text{CaO}_3:\text{Eu}^{3+}$ preparation is started by mixing all materials within water or methanol to form a slurry. After thoroughly mixing, leave the slurry to be dried in air conditioning and pulverize the substance to get a powder form. It will be put into specific containers for burning three times, and after each firing stage finishes, it will be re-powdered. It is noted that the condition of each combustion phase is different. Particularly, the first one is carried out with the powder placed in closed quartz pipes filled with N_2 , under a temperature of 1200°C , and lasts for two hours. In the second combustion, an open capped quartz boat is used, the N_2 loaded with H_2O is put inside the boat, and the temperature remains 1200°C for 1 hour. The product is quenched to room temperature as quickly as possible before being powdered. The last combustion stage is carried out for approximately 20 minutes with stagnant air flowing into the open capped quartz boat at 1200°C . The product is quenched to room temperature again before being ground into powder. The powder is then stored in a tightly sealed container that is kept dry. The optical features of this $\text{CaO}_3:\text{Eu}^{3+}$ are emitting red emission and mainline emission peak at 2.0.15 eV. In terms of the green phosphor $\text{Zn}_2\text{SiO}_4:\text{Mn}^{2+}$, the mixing process of all the ingredients is carried out by ball-milling in the water for approximately 2 hours. After that, the mixture is then air dried and turned into a powder. It will be heated twice within open quartz containers, under a temperature of 1200°C , within 1 hour. Yet, the first time, the forming gas is filled into the containers, while the airflow is used the second time. After the first combustion, it is very important to powderize the product before starting the second combustion. The characteristics of the green phosphor $\text{Zn}_2\text{SiO}_4:\text{Mn}^{2+}$ are green radiation color, 2.35 eV radiation peak and 0.18 eV radiation width.

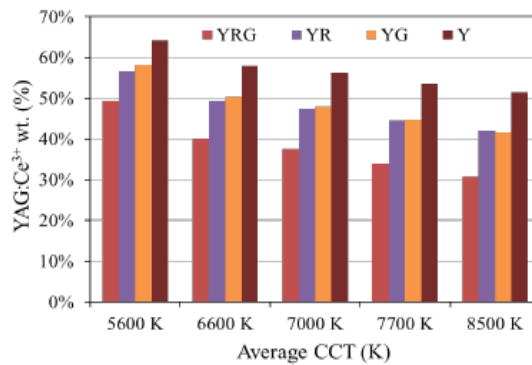


Figure 2 The phosphor $\text{YAG}:\text{Ce}^{3+}$ content within dissimilar remote phosphor structures and color ACCTs

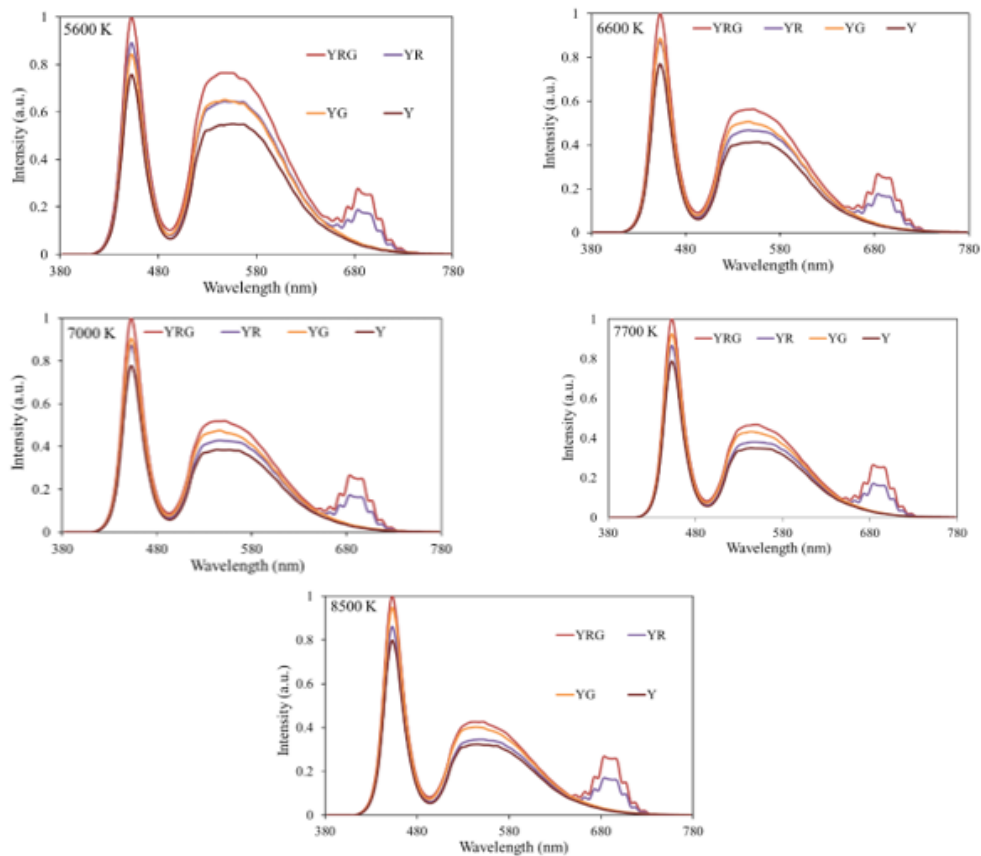


Figure 3 Discharge spectra for each distant phosphor configuration at distinct ACCTs

To better understand the influence of phosphor concentrations on the lighting properties of the distant phosphor packages, the changes in YAG: Ce^{3+} phosphor concentration in each distant configuration following dissimilar CCTs are investigated and demonstrated in Figure 2. Can be seen easily, at all CCTs, the yellow phosphor concentration shows its maximum level in single-layer Y configuration and minimum level in triple-layer YGR configuration, while the figures in dual-layer YR and YG are relatively the same. In general, given that all structures were designed with a similar CCT value, the structure with the higher concentration of yellow YAG: Ce^{3+} will have a lower luminous flux because the phosphor packages have more backscattering events. In addition, the greater concentration of yellow phosphor means a color distribution imbalance and lower color uniformity. Thus, it appears that the YGR can yield the highest luminescence and chromaticity performance for WLED packages.

According to the general concepts, the higher chromatic homogeneity and color rendering index (CRI) could be achieved with the red-spectral enrichment in the spectral range of the generated white lighting. Regarding luminescence, adding the green spectral region probably offers an effective control. Therefore, it is essential to investigate the radiation spectra of each remote phosphor structure at specific CCTs to examine their influences on the hue standard and illuminating efficiency of WLEDs. Figure 3 illustrates the measured results of emission spectra at the CCT of 5600 K, 6600 K, 7000 K, 7700 K, and 8500 K.

The radiation spectra of the Y structure are the lowest, meaning the hue standard and lumen productivity of the single-layer structure are inferior to those of the others. In contrast, regardless of CCTs, the triple-layer remote phosphor (YGR) is superior as it emits the maximum spectral strength in the visible light wavelength band (380 nm - 780 nm). Besides, between the two dual-layer structures, in the green wavelength range between

500 nm and 570 nm, the YG has greater emission intensity than the YR, which indicates that the YG can yield better luminous flux. Meanwhile, in the wavelength of red color, 650 nm – 750 nm, the YR gives greater values. Thus YR is more beneficial to the color quality, especially the CRI of a WLED. To verify these findings, the calculations based on Mie’s hypothesis and Beer’s law, which are useful and effective tools, are particularly demonstrated in the following section.

3. Results and Discussion

Figure 4 clearly shows the CRI of each remote phosphor configuration. The YR apparently provided the highest CRI at all five CCTs. Meanwhile, the YG resulted in the lowest CRI. This noticeable CRI improvement of the YR structure can be attributed to the red phosphor $\text{CaO}_3:\text{Eu}^{3+}$ function promoting the red spectral intensity, which is advantageous to the CRI. In addition, the YR has increased the CRI of either the low CCT or the high CCT WLED packages. Since the CRI enhancement in high CCT WLED (for example, 8500 K) confronts tremendous difficulties, this result has become significantly important to the application of dual-film distant phosphor configurations for further development of WLED devices. As mentioned above, the color quality will be analyzed via two parameters: the CRI (which has already been presented) and CQS. Figure 5 shows the CQS functions for all four structures. Though the CRI of the triple-layer YGR is lower than the YR, its CQS has the highest value. The color quality scale has been investigated recently. Researchers have pointed out that CQS is more powerful than the CRI as it evaluates the color performance based on three different parameters of CRI, human visual preference and the color coordinate. That the YGR can yield the highest CQS correlates with the uniform color distribution for three primary colors: blue, red, and green. In addition, the higher CQS leads to better chromaticity for the acquired light in white. Hence, the three-sheet YGR layout has turned out to be the most potential to enhance the color quality of the WLED packages. On the other hand, the Y structure has the lowest CQS as its spectral band lacks both green and red elements, leading to poor uniformity in color performance. However, the advantage of the single-layer over the other structures is its simpler and easier fabrication, which helps to reduce production costs significantly.

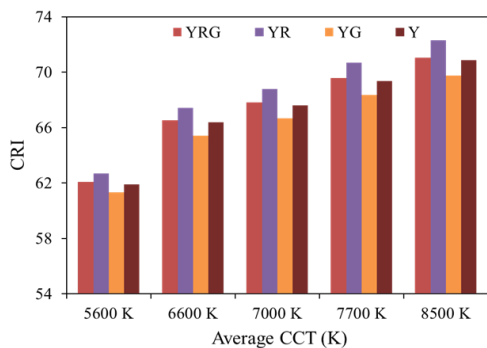


Figure 4 Hue rendering index values of each remote phosphor structure at different ACCTs

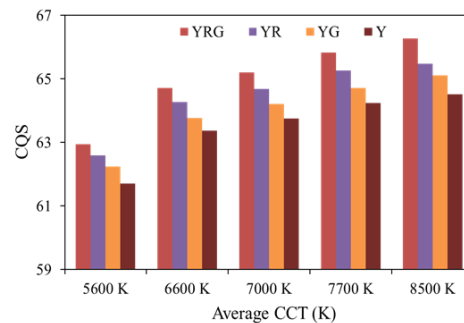


Figure 5 Hue standard scale of each remote phosphor structure at different ACCTs

Based on the findings above, the YGR is an excellent option to enhance the color quality of WLED since its CRI and CQS are higher than the original one (the single Y structure). As previous studies mentioned that the enhancing hue standard is accompanied by decreased lumen productivity. Therefore, the question is whether the YGR suffers the same phenomenon or whether it is possible to improve color uniformity and luminescence simultaneously.

The similitude of the illuminating beam among the triple-film, dual-film, and single-film structures should be drawn to figure out the answer. We presented the mathematic model based on the theory of Mie scattering (Li et al., 2010; Liu et al., 2010; Irawan et al., 2017) for the task of assessing the transferred blue lights as well as transformed yellow lights for the single-film, two-film, and triple-film models. The computed outcomes prove the effectiveness of using more phosphor layers in a WLED remote structure for higher lighting efficiency. In the single-film structure with the phosphor film’s thickness of $2h$, the computation of transformed yellow light and the transferred blue light can be defined as:

$$PB_1 = PB_0 \times e^{-2\alpha_{B_1}h} \tag{1}$$

$$PY_1 = \frac{1}{2} \frac{\beta_1 \times PB_0}{\alpha_{B_1} - \alpha_{Y_1}} (e^{-2\alpha_{Y_1}h} - e^{-2\alpha_{B_1}h}) \tag{2}$$

Meanwhile, in the dual-film configuration, the phosphor layer is h thick, and the transformed yellow illumination, as well as the transferred blue illumination, can be calculated as follows:

$$PB_2 = PB_0 \times e^{-2\alpha_{B_2}h} \tag{3}$$

$$PY_2 = \frac{1}{2} \frac{\beta_2 \times PB_0}{\alpha_{B_2} - \alpha_{Y_2}} (e^{-2\alpha_{Y_2}h} - e^{-2\alpha_{B_2}h}) \tag{4}$$

The enhancement in optical efficacy of the dual-sheet layout will be obvious when compared to the effectiveness of the single-film layout, as follows:

$$\frac{(PB_2+PY_2)-(PB_1+PY_1)}{PB_1+PY_1} > 0 \tag{5}$$

Then, for comparison among the dual-film and triple-film performance, the calculation of the transferred blue illumination and transformed yellow illumination can be performed as the following expressions. For the double-layer configuration which has the phosphor film has a $2h$ thickness, the blue illumination transferred as well as transformed yellow illumination will be:

$$PB_2 = PB_0 e^{-\alpha_{B_2}h} e^{-\alpha_{B_2}h} = PB_0 e^{-2\alpha_{B_2}h} \tag{6}$$

$$\begin{aligned} PY_2 &= \frac{1}{2} \frac{\beta_2 PB_0}{\alpha_{B_2} - \alpha_{Y_2}} [e^{-\alpha_{Y_2}h} - e^{-\alpha_{B_2}h}] e^{-\alpha_{Y_2}h} + \frac{1}{2} \frac{\beta_2 PB_0}{\alpha_{B_2} - \alpha_{Y_2}} [e^{-\alpha_{Y_2}h} - e^{-\alpha_{B_2}h}] \\ &= \frac{1}{2} \frac{\beta_2 PB_0}{\alpha_{B_2} - \alpha_{Y_2}} [e^{-2\alpha_{Y_1}h} - e^{-2\alpha_{B_1}h}] \end{aligned} \tag{7}$$

Those lights from the three-sheet layout having $\frac{2h}{3}$ the breadth for one phosphor layer can be calculated as follows:

$$PB_3 = PB_0 \cdot e^{-\alpha_{B_2} \frac{2h}{3}} \cdot e^{-\alpha_{B_2} \frac{2h}{3}} \cdot e^{-\alpha_{B_2} \frac{2h}{3}} = PB_0 \cdot e^{-2\alpha_{B_3}h} \tag{8}$$

$$\begin{aligned}
 PY'_3 &= \frac{1}{2} \frac{\beta_3 PB_0}{\alpha_{B_3} - \alpha_{Y_3}} [e^{-\alpha_{Y_3} \frac{2h}{3}} - e^{-\alpha_{B_3} \frac{2h}{3}}] e^{-\alpha_{Y_3} \frac{2h}{3}} + \frac{1}{2} \frac{\beta_3 PB_0 e^{-\alpha_{B_3} \frac{2h}{3}}}{\alpha_{B_3} - \alpha_{Y_3}} \\
 &\quad [e^{-\alpha_{Y_3} \frac{2h}{3}} - e^{-\alpha_{B_3} \frac{2h}{3}}] \\
 &= \frac{1}{2} \frac{\beta_3 PB_0}{\alpha_{B_3} - \alpha_{Y_3}} [e^{-\alpha_{Y_3} \frac{4h}{3}} - e^{-2\alpha_{B_3} \frac{4h}{3}}]
 \end{aligned} \tag{9}$$

$$\begin{aligned}
 PY_3 &= PY'_3 \cdot e^{-\alpha_{Y_3} \frac{2h}{3}} + PB_0 \cdot e^{-2\alpha_{B_3} \frac{4h}{3}} \frac{1}{2} \frac{\beta_3}{\alpha_{B_3} - \alpha_{Y_3}} [e^{-\alpha_{Y_3} \frac{2h}{3}} - e^{-\alpha_{B_3} \frac{2h}{3}}] \\
 &= \frac{1}{2} \frac{\beta_3 PB_0}{\alpha_{B_3} - \alpha_{Y_3}} [e^{-\alpha_{Y_3} \frac{4h}{3}} - e^{-\alpha_{B_3} \frac{4h}{3}}] e^{-\alpha_{Y_3} \frac{2h}{3}} + \frac{1}{2} \frac{\beta_3 PB_0 e^{-\alpha_{B_3} \frac{4h}{3}}}{\alpha_{B_3} - \alpha_{Y_3}} \\
 &\quad [e^{-\alpha_{Y_3} \frac{2h}{3}} - e^{-\alpha_{B_3} \frac{2h}{3}}] \\
 &= \frac{1}{2} \frac{\beta_3 PB_0}{\alpha_{B_3} - \alpha_{Y_3}} [e^{-\alpha_{Y_3} h} - e^{-2\alpha_{B_3} h}]
 \end{aligned} \tag{10}$$

As shown by the following equations, the triple-layer structure can provide better lighting performance than the dual-layer structure.

$$\frac{(PB_3 - PY_3) - (PB_2 + PY_2)}{(PB_2 + PY_2)} > \frac{e^{-2\alpha_{B_3} h} - e^{-2\alpha_{B_2} h}}{e^{-2\alpha_{Y_3} h} - e^{-2\alpha_{B_2} h}} > 0 \tag{11}$$

Here, in the equations from (1) to (11), h is the breadth of one phosphor's sheet from each remote phosphor configuration. The subscripts "1", "2", and "3" define the single-film, dual-film, and triple-film structures, respectively. β indicates the transformation factor of the blue illumination transformed into yellow illumination. γ presents the reflection factor for the yellow illumination. αB and αY describe the power lost proportions for blue and yellow light throughout their spreading within the phosphor film. PB and PY show the blue illumination strength and yellow illumination strength. PB_0 (containing PB and PY) indicates the illumination strength from the LED chip. Besides, PY_3 from Equation (4) presents the yellow illumination transferred via the red and green phosphor layers. The Mie hypothesis would also be employed to analyze the dispersal proficiency for the phosphor materials and assess the dispersal cross-section C_{sca} of the phosphor spheres (Nguyen et al., 2021b). Additionally, we utilized the law of Lambert-Beer to assess the transferred optical energy as follows:

$$I = I_0 \exp(-\mu_{ext}L) \tag{12}$$

I_0 signifies the incident power, while L and μ_{ext} are the thickness of phosphor films and the extinction factor, in turn. μ_{ext} is assessed via $\mu_{ext} = Nr \cdot C_{ext}$, in which Nr signifies the number density allocation for granules (mm⁻³), and C_{ext} (mm²) signifies the extinction crosssection for the spherical phosphors.

According to Equations (5) and (11), using the triple-film YGR to increase the luminous flux of the WLED package is more efficient than using the dual- and single-film designs. This is illustrated in Figure 6, where the YGR structure produces the most lumens regardless of color temperature. Meanwhile, the Y configuration had the lowest luminous value. Besides, the dual-layer applying green phosphor Zn₂SiO₄:Mn²⁺ layer (YG) shows a noticeable control over the luminous efficiency as its luminescence is lower than the YGR. The increase of green power in the 500 nm – 570 nm region of white-light spectra could demonstrate this

luminescent improvement, as shown in Figure 3. As can be seen, the green spectral region in YGR has a higher intensity than that in YG, YR, and Y; therefore, the luminous flux of YGR is better than the others. Furthermore, as shown in Figure 2, the YAG:Ce³⁺ content from the YGR is the lowest, which is not only effective in maintaining the stable CCT but also essential to initiating considerable scattered-light reduction, along with better blue-light transmission and energy conversion. Therefore, the light trapped and circulated inside the package is effectively reduced, increasing the light extraction efficiency of the WLED structure. As a result, YGR has the most excellent luminous efficacy.

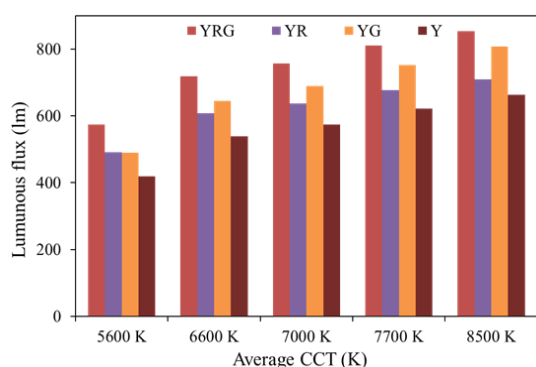


Figure 6 Lumen output of each remote phosphor configuration at different ACCTs

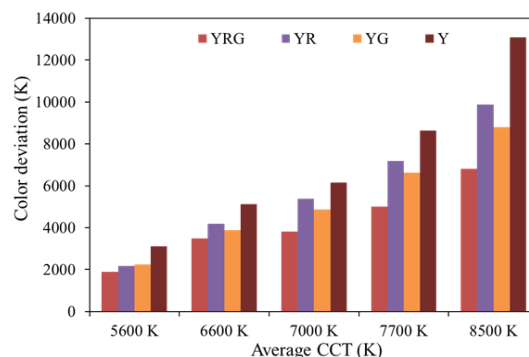


Figure 7 The color deviations (CDs) of each distant phosphor structure at different ACCTs

Triple-layer structure YGR can be the most suitable solution to achieve considerable improvements in CQS and lumen output of WLED. Nevertheless, we should consider the color copper to verify this structure's effectiveness in bettering the color quality of WLEDs. Various methods were proposed for higher color copper, including using SEPs such as SiO₂ and CaCO₃ or conformal coating structure, but the luminous output was degraded considerably. In the case of using the YGR structure, there are advantages to both color homogeneity and luminescence. Particularly, the green phosphor Zn₂SiO₄:Mn²⁺ and red phosphor CaO: Eu³⁺ can add green light components and red light ones, thereby increasing scattering property and distributing color components more uniformly. In addition, the remote phosphor structure minimized a large proportion of light reflected by the LED chip, resulting in higher light transmission that benefits the luminous output. Nevertheless, it is advisable to adjust the phosphor sheets' content for the task of obtaining the maximal level of power transference, as demonstrated by Equation (12), which applies the Lambert-Beer law.

The authors investigated the color deviation (CD) in each structure to have more concrete proof of the ability of the YGR layout to increase hue output for a WLED lamp. Figure 7 portrays the CD measurement results for each remote phosphor model. It can be seen that the level of DC in YGR is the lowest in all CCTs. The enhancement in scattering properties of the YGR structure may be the driving force behind this development in color quality. It can be explained that more phosphor layers cause more light scattering, which leads to better light mixing before generating white light. Thus, the light becomes more homogenous. Even so, the increase in diffusing time means a decrease in illuminating intensity. Yet, this reduction is a minor and acceptable drawback as it is possible to augment the hue output. The lumen also remains at a high level when using the YGR structure. Thus, manufacturers can improve the quality of their WLED products by using this triple-film distant phosphor configuration.

4. Conclusions

The comparison of lighting performance among the triple-layer (YGR), dual-layer (YG and YR), and single-layer (Y) are provided in this article to figure out the most suitable remote phosphor structure for further WLED developments. WLED models are simulated using green $\text{Zn}_2\text{SiO}_4:\text{Mn}^{2+}$ and red $\text{CaO}:\text{Eu}^{3+}$. Mie's hypothesis and Beer's law would be utilized to investigate and validate the measured outcomes. The findings indicate that the YR is advantageous to the CRI of the WLED as the red phosphor helps to increase the red components in the white-light spectral region. At the same time, the YG is suitable for the luminous flux due to the rise in the green spectral intensity. Despite ranking second in terms of CRI, the YGR has the highest value in CQS and luminous efficacy regardless of CCTs. Moreover, the color deviation in YGR is the smallest, implying that the color uniformity in YGR is the highest. Therefore, YGR is the superior remote structure that can be used for higher quality WLED creation.

Acknowledgements

This research is supported by the Industrial University of Ho Chi Minh City (IUH) under grant number 121/HD-DHCN.

References

- Agarwal, S., Haseman, M.S., Khomehchi, A., Saadatkia, P., Winarski, D.J., Selim, F.A., 2017. The Physical and Optical Properties of Ce: YAG Nanophosphors and Transparent Ceramics and the Observation of Novel Luminescence Phenomenon. *Optical Materials Express*, Volume 7, pp. 1055–1065
- Anh, N.D.Q., Vinh, N.H., Lee, H.Y., 2017a. Effect of Red-emitting $\text{Sr}_{2.41}\text{F}_{2.59}\text{B}_{20.03}\text{O}_{74.8}:\text{Eu}_{0.12}, \text{Sm}_{0.048}$ Phosphor on Color Rendering Index and Luminous Efficacy of White LEDs. *Current Optics and Photonics*, Volume 1(2), pp. 118–124
- Anh, N.D.Q., Vinh, N.H., Lee, H.Y., 2017b. Gaussian Decomposition Method in Designing a Freeform Lens for an LED Fishing/Working Lamp. *Current Optics and Photonics*, Volume 1(3), pp. 233–238
- Anh, N.D.Q., Ngoc, H.V., 2020. Building Superior Lighting Properties for WLEDs Utilizing Two-Layered Remote Phosphor Configurations. *Materials Science-Poland*, Volume 38, pp. 493–501
- Cheng, J., Zhang, J., Lu, J., Bian, X.T., Zhang, H.C., Shen, Z.H., Ni, X.W., Ma, P.C., Shi, J., 2019. Photoluminescence Properties of $\text{Ca}_4\text{La}_6(\text{SiO}_4)_4(\text{PO}_4)_2\text{O}_2$ -Based Phosphors for wLEDs. *Chinese Optics Letters*, Volume 17(5), p. 051602
- Davis, W., Ohno, Y., 2010. Color Quality Scale. *Optical Engineering*, Volume 49(3), p. 033602
- Ding, X.R., Chen, Q., Tang, Y., Li, J.S., Talwar, D.P., Yu, B.H., Li, Z.T. 2018. Improving the Optical Performance of Multi-Chip LEDs by using Patterned Phosphor Configurations. *Optics Express*, Volume 26(6), pp. A283–A292
- Gao, W.J., Ding, K., He, G.X., Zhong, P., 2018. Color Temperature Tunable Phosphor-Coated White LEDs with Excellent Photometric and Colorimetric Performances. *Applied Optics*, Volume 57, pp. 9322–9327
- Ge, Z., Piquette, A., Mishra, K.C., Klotzkin, D., 2015. Enhanced Forward Emission of YAG: Ce^{3+} Phosphor with Polystyrene Nanosphere Coating. *Applied Optics*, Volume 54, pp. 6025–6028
- Irawan, Y., Juliana, I., Adilina, I.B., Alli, Y.F., 2017. Aqueous Stability Studies of Polyethylene Glycol and Oleic Acid-Based Anionic Surfactants for Application in Enhanced Oil

- Recovery through Dynamic Light Scattering. *International Journal of Technology*. Volume 8(8), pp. 1414–1421
- Jiang, P.Q., Peng, Y., Mou, Y., Cheng, H., Chen, M.X., Liu, S., 2017. Thermally Stable Multicolor Phosphor-In-Glass Bonded on Flip-Chip UV-LEDs for Chromaticity-Tunable WLEDs. *Applied Optics*, Volume 56, pp. 7921–7926
- Li, B., Zhang, D.W., Huang, Y., Ni, Z., Zhuang, S., 2010. A New Structure of Multi-Layer Phosphor Package of White LED with High Efficiency. *Chinese Optics Letters*, Volume 8(2), pp. 221–223
- Li, J.S., Chen, Y.H., Li, Z.T., Yu, S.D., Tang, Y., Ding, X.R., Yuan, W. 2016. ACU Optimization of pcLEDs by Combining the Pulsed Spray and Feedback Method. *Journal Display of Technology*, Volume 12(10), pp. 1229–1234
- Liu, Z., Liu, S., Wang, K., Luo, X., 2010. Measurement and Numerical Studies of Optical Properties of YAG: Ce Phosphor for White Light-Emitting Diode Packaging. *Applied Optics*, Volume 49(2), pp. 247–257
- Luo, G.F., Loan, N.T.P., Tho, L.V., Anh, N.D.Q., Lee, H.Y., 2020. Enhancement Of Color Quality and Luminous Flux for Remote-Phosphor Leds with Red-Emitting $\text{CaMgSi}_2\text{O}_6:\text{Eu}^{2+}$, Mn^{2+} . *Materials Science-Poland*, Volume 38, pp. 409–415
- Nguyen, T.M.H., Ton, T.P., Anh, N.D.Q., 2021a. Eu-Activated Strontium-Barium Silicate: A Positive Solution for Improving Luminous Efficacy and Color Uniformity of White Light-Emitting Diodes. *Materials Science-Poland*, Volume 38, pp. 594–600
- Nguyen, T.M.H., Ton, T.P., Anh, N.D.Q., Thanh T.T., 2021b. Triple-layer remote phosphor structure: a novel option for enhancing WLEDs' color quality and luminous flux" *Materials Science-Poland*, Volume 38(3), pp. 654–660
- Sulistiyanto, N., Rifan, M., Setyawati, O., 2014. Development of a 20V-LED Driver Based on the Boost Converter using an FPGA Module. *International Journal of Technology*, Volume 5(3), pp.287–292
- Ton, T.P., Phuong, L.N.T., Le, V.T., Anh, N.D.Q., Liao, H.Y., Luo, G.F., Lee, H.Y., 2021. Enhancing Color Quality of WLEDs with Dual-Layer Remote Phosphor Geometry. *Materials Science- Poland*, 38(4), pp. 667–674
- Widiyati, C., Poernomo, H., 2018. Design of a Prototype Photoreactor UV-LEDs for Radiation Vulcanization of Natural Rubber Latex. *International Journal of Technology*. Volume 9(1), pp. 130–141
- Yang, L., Zhang, Q., Li, F., Xie, A., Mao, L., Ma, J.D. 2019a. Thermally Stable Lead-Free Phosphor in Glass Enhancement Performance of Light Emitting Diodes Application. *Applied Optics*, Volume 58(15), pp. 4099–4104
- Yang, X., Chai, C.F., Chen, J.C., Zheng S.S., Chen, C., 2019b. Single 395 nm Excitation Warm WLED with a Luminous Efficiency of 104.86 lm/W and a Color Rendering Index of 90.7. *Optical Materials Express*, Volume 9(11), pp. 4273–4286
- Yuce, H., Guner, T., Balci, S., Demir, M.M., 2019. Phosphor-Based White LED by Various Glassy Particles: Control Over Luminous Efficiency. *Optics Letters*, Volume 44(3), pp. 479–482
- Zhang, J., Ji, B.W., Hua, Z.H., 2016. Investigations on the Luminescence of $\text{Ba}_2\text{Mg}(\text{PO}_4)_2:\text{Eu}^{2+}$, Mn^{2+} Phosphors for LEDs. *Optical Materials Express*, Volume 6(11), pp. 3470–3475